Science Signaling Manuscript Template

General Instructions on using this template and submitting a manuscript to *Science Signaling*: Using this template will help to speed the processing of your paper. Our goal is to be able to identify each section of your manuscript so that we can accurately record the title, authors, abstract, etc. and also be able to enrich it by including reference links and an accurate layout.

Please use the actual template, which starts on page 2. When you are ready to submit, please delete the text on this cover page.

You can submit your paper at www.submit2scisignal.org
Additional instructions are available at http://stke.sciencemag.org/about/help/research.dtl

Specific formatting instructions are provided in the actual template, which follows.

Title: The COPI/II adaptor protein TMED7 is required to initiate and regulate anterograde trafficking of the immunoreceptor TLR4

Authors: Ardi Liaunardy-Jopeace[1], Clare E. Bryant[2] and Nicholas J. Gay[1]*

One Sentence Summary: We elucidate the mechanism by which TLR4 is trafficked in the early secretory pathway and how this is coupled to inflammatory signaling.

Affiliations:

[1]Dept Biochemistry, University of Cambridge, 80, Tennis Court Rd., Cambridge, CB2 1GA, UK.

[2] Dept Veterinary Medicine, University of Cambridge, Madingley Rd, Cambridge, UK

* To whom correspondence should be sent

email: njg11@cam.ac.uk

phone: +44 1223 334976

fax: +44 1223 766002

The bacterial endotoxin receptor TLR4 is subject to multiple points of regulation at the level of signalling, biogenesis and trafficking. Dysregulation of the pathway can cause serious autoimmune diseases such as sepsis. Here we report that the p24/emp family protein TMED7 controls the trafficking of TLR4 from the Golgi to the cell surface. TMED7 is able to form a stable complex with the ectodomain of TLR4, an interaction that requires the coiled-coil and GOLD domains but not the cytosolic COP II sorting motif of TMED7. Depletion of TMED7 reduced MyD88 but not TRAM/TRIF dependent signaling through the TLR4 pathway. Truncated forms of TMED7 that lack the COP II sorting motif or transmembrane domain are mislocalized and can cause constitutive activation of the TLR4 signalling pathways. Overall these results support the hypothesis that p24 proteins act as a quality control step by recognising correctly folded anterograde cargo in the early secretory compartments and positively regulate the translocation of cargo such as TLR4 to the cell surface.

INTRODUCTION

The Toll-like receptor 4 (TLR4) is a key regulator of innate immunity and inflammation. It is activated by the complex and heterogenous glycolipid lipolysaccharide (LPS) present in the outer membrane of Gram –ve bacteria (*1*). Although TLR4 is a key element of host defence against Gram -ve pathogens, dysregulation of this signal transduction pathway causes endotoxic shock, a severe condition that leads to multi-organ failure and death. Because of its importance in innate immunity and disease the activity of TLR4 is highly regulated not only by positive and negative effectors of the signal transduction pathway but also at the level of biosynthesis and trafficking.

TLR4 functions at the cell surface and also signals from early endosomes (*2, 3*). The trafficking events that accompany activation of TLR4 are fairly well understood. Stimulation of TLR4 by LPS induces internalization of the receptor into early endosomes, a process that requires the accessory protein CD14, the GTPase Rab and potentially signalling by the Syk tyrosine kinase (*4-6*). TLR4 is unusual as it promotes two signalling pathways via MyD88 leading to activation of NF-κB and proinflammatory responses and through the TRAM and TRIF adaptors to the activation of interferon response factors (IRF3 and 7) (*7*). The evidence suggests that the latter pathway is only active after internalization. By contrast the trafficking processes that accompany biosynthesis are less well characterized. Two chaperone molecules gp96 and PRAT4 are required for proper processing of TLR4 in the ER that leads to the secretion of the receptor to the plasma membrane (*8-10*). Association of TLR4 with MD2 in the ER is also crucial for correct glycosylation, secretion to the plasma membrane, and hence LPS responsiveness (*11-14*). The involvement of other components of the secretory pathway, especially those related to vesicular trafficking, is however relatively unknown. A recent study has shown that Rab10 is responsible for transporting TLR4 from the Golgi to the plasma membrane upon LPS stimulation (*15*).

Secretion of cell surface transmembrane proteins is initiated by translocation and folding of the protein in the ER. Proteins destined for secretion rather than ER residence are then selectively packaged into vesicles for transport to the cis-Golgi. This process is dependent on the ability of the cargo protein to recruit COP II coat protein complexes that leads to their assembly around the budding membrane prior to vesicle formation (*16*). This recruitment is mediated by the presence of COP II-binding motif of di-phenylalanine in the cytosolic tail of the cargo

protein (*17-19*). However soluble cargo proteins and indeed many transmembrane proteins including TLR4 do not have this cytosolic diphenylalanine signal. Instead these cargo molecules are selected by transmembrane adaptor proteins that have recognition domains exposed in the ER lumen and short cytoplasmic tails that include the diphenylalanine sorting motif for COP II and a dibasic signal for COP I dependent retrograde transport back to the ER from the Golgi (*20*).

One important family of transmembrane adaptor proteins are the p24 proteins, alternatively called TMED (transmembrane emp24 protein transport domain containing) in vertebrates. There are ten family members in mammals and they are very highly conserved across species. TMEDs consist of luminal golgi dynamics (GOLD) and coiled coil domains in the lumen, a single transmembrane spanning region and a short cytosolic tail with COP II and/ or COP I sorting signals (*21, 22*). TMEDs form homo and hetero dimers and are found in the early secretory pathway of the ER, ER golgi intermediate compartment (ERGIC), the cis-Golgi, and COP I and II-coated vesicles (*19, 23-26*). In yeast, deletion of several p24 proteins leads to defects in secretion of several proteins and in formation of secretory vesicles, and activation of the unfolded protein response (UPR), but is not lethal (*27-29*). In mouse, deletion of certain TMEDs leads to defective embryogenesis that can be lethal (*30, 31*). Although it is clear that TMEDs have a fundamental cell biological function in the selection of secretory cargo little is known about the nature of the cargo molecules or the molecular mechanisms by which these molecules are recognized in the ER and dissociated in the Golgi (*22*).

In this paper we show that the pattern recognition receptor TLR4 is a cargo molecule for TMED7 which tightly regulates trafficking of the receptor to the cell surface. Dysregulation of TMED7- mediated transport leads to potentially dangerous constitutive activation of the TLR4 signalling pathway.

RESULTS

TMED7 is a type I membrane protein with a luminal N-terminal Golgi Dynamics (GOLD) domain.

Previous reports have suggested that TMED7 is localized on the cytosolic surface of the membrane (*32*). However those studies contradict bioinformatic analysis that predicts TMED7 to be a secreted membrane protein with a type I topology, and a short cytosolic domain at the C-terminus (Figs. 1A, C, S1A, and B). In order to resolve this issue we asked whether TMED7

contains N-linked glycans and disulphide bonds, post-translational modifications that are added to the protein in the lumen of the endoplasmic reticulum during biosynthesis. Treatment of cell extracts with the glycosidase PNGaseF leads to the formation of a faster migrating species of TMED7-FLAG (Fig. 1B). This shows that TMED7 is glycosylated most likely at asparagine 103 in the GOLD domain, the only predicted N-linked glycosylation site found in the protein with the consensus sequence of Asn-Xaa-Thr, which is absolutely conserved in TMED7 across various species (Fig. S1C). A similar outcome was seen in TLR4, which is heavily glycosylated, but not in TRAM which is not glycosylated (Fig. S2A). This finding confirms the observation made by Fullekrug (*24*). Multiple sequence alignment of p24 proteins reveals that there are two absolutely conserved cysteine residues within the GOLD domain that may be involved in the formation of a disulphide bridge (*21*). To test this hypothesis, we expressed TMED7-HA in HEK293T cells and analyzed the protein under reducing and non-reducing conditions. Under non-reducing conditions TMED7 migrates faster, a characteristic of the oxidized denatured state (Fig. 1B). Finally, recombinant human TMED7 proteins with its native or fusion signal peptide (SP-CC and PP-CC, respectively) were expressed in insect cells and analyzed by Edman degradation which revealed that a hydrophobic N-terminal signal sequence had been cleaved before residue serine 35 (*19*, Fig. S2B and C). Taken together this evidence supports the membrane topology for TMED7 shown in Fig 1C.

TMED7 oligomers interact with TLR4 in the Golgi

We next asked whether TMED7 is able to dimerize or oligomerize with itself and interact with TLR4. Three truncated constructs of TMED7 were generated with C-terminal HA or FLAG tag (Fig. 2A) and transfected into HEK293T cells. FLAG-tagged protein was immunoprecipitated and anti HA antibody was used to detect any HA-tagged protein that formed complexes. TMED7, Delta, and CC can form an oligomer between themselves and each other, but not GOLD (Figs. 2B and D). This shows that the coiled-coil domain, which is lacking in the GOLD construct, is required for oligomerization. Fusion proteins expressed in THP-1 macrophages by lentiviral transduction also showed that TMED7 was able to oligomerize with itself and that it requires the coiled-coil domain for function (Fig. S3A).

To test whether TLR4 interacts with TMED7 and the truncation mutants, HEK293T cells were transfected with FLAG-TLR4, CD14, MD2, and TRAM-FLAG (TLR4 complex) along with HA-tagged TMED7 or its truncated mutants. FLAG-tagged protein was immunoprecipitated and anti-HA antibody was used to detect associated protein. We found that TMED7, Delta, and CC were co-immunoprecipitated with the TLR4 complex but the construct lacking the coiled-coil motif (GOLD) was not (Fig. 2C and D). TLR3, however, did not interact with TMED7 (Fig. S3B). Treatment with 100 ng/ml LPS reduced the amount of full length TMED7 but not CC bound to TLR4 (Fig. 2C). This suggests that LPS stimulation might trigger the dissociation of TLR4 from TMED7.

Confocal microscopy analysis using unstimulated HEK293T cells revealed that the interaction between TLR4 and TMED7 occurred in the Giantin-positive intracellular compartment, which is an organelle marker for the Golgi (Fig. 3). In transduced THP-1 macrophages TLR3 did not co-localize with TMED7 in the Golgi, which suggests that TMED7 may recognize TLR4 specifically (Fig. S6A). Together, these data indicate that the coiled-coil domain of TMED7 mediates homo- or hetero- dimerization and that TLR4 binds to dimeric TMED7 in the Golgi in the unstimulated state.

TMED7 modulates TLR4 signalling

The results above suggest that TMED7 recognizes TLR4 in the ER as cargo for transport to the Golgi. We therefore asked whether depletion of TMED7 affected LPS induced signalling by TLR4. TMED7 transcript is expressed in both HEK293 cells and the THP-1 macrophages (Fig 4A). Transfection of HEK293 cells and THP-1 macrophages with gene-specific siRNAs resulted in a substantial reduction in gene expression of TMED7 but a scrambled control siRNA had no effect (Fig 4B). Depletion of TMED7 with siRNA reduced IL-6 and TNFα production, but not RANTES, in THP-1 macrophages stimulated with LPS (Fig. 4C). Luciferase reporter assays performed in transfected HEK293 cells showed that TMED7 knockdown by siRNA reduced NF-κB but not IFNβ activation upon TLR4 stimulation by LPS providing further evidence that only the MyD88-dependent pathway is affected by TMED7 knockdown (Fig. S4A and B). By contrast depletion of TMED7 did not affect TLR3 and TLR5 signalling induced by Poly I:C and flagellin, respectively (Fig. S4C and D).

We also performed the reciprocal assay by over-expressing TMED7 to see whether signalling was enhanced. As the amount of TMED7 transfected into HEK293 cells was increased, the basal signalling level in the absence of LPS increased for both MyD88 and TRIF/TRAM pathways. By contrast LPS induced signalling was unaffected by the overexpression (Fig. 5B and C). This shows that TMED7 acted upstream of TLR4 activation by LPS. The responses seen in this assay were specific for LPS induced TLR4. GOLD overexpression did not cause similar increase in TLR4 constitutive activity. Thus this effect is not caused by the transfection of foreign DNA plasmid (Fig. S5A and B). Moreover, both NF-κB and IFNβ luciferase activity is dependent on the presence of all TLR4 signalling components (Fig. S5C, D, and E). Lastly, TMED7, Delta, and CC did not alter the activity of TLR3 and 5 upon their stimulation in transiently transfected HEK293 cells (Fig. S5G and H). Altogether, this suggests that TMED7 can promote ligand-independent activation of TLR4 signalling. To explore this finding further, we determined which components of the TLR4 receptor complex are required to interact with TMED7. Co-immunoprecipitation experiments show that TLR4 on its own or in combination with co-receptors CD14 and MD-2 can interact with TMED7. Although the TLR4 adaptor TRAM is not able to associate with TMED7, it substantially enhances TMED7 binding to the TLR4 complex and TLR4 alone (Fig. 5A, lane 3, 4, 7, 8, and 9).

Regulatory roles of the cytoplasmic tail and transmembrane domain of TMED7 in TLR4 signalling

Previous studies have shown that COP-I and II binding motifs in the cytoplasmic tail, as well as the conserved E and Q residues in the transmembrane domain of p24 proteins determine the direction of trafficking and the rate of recycling of the proteins within the early secretory pathway (*17, 19, 33*). We therefore investigated whether these would affect TLR4 signalling. To study this, we used the truncated mutants described above (Fig. 2A). Expression of delta mutant increased constitutive signalling through the MyD88 and TRIF/TRAM pathways by about 20-fold but a residual level of LPS-inducible signalling was also detected (Fig. 6A and B). The effect seen here was greater than that of full length TMED7 (compare to Fig. 5B and C). CC expression also enhanced constitutive activity of both pathways to a similar level to that of full length TMED7 (Fig. 6C and D), whereas GOLD overexpression did not have any effect, as expected since this truncation does not interact with TLR4 (Fig. S5A and B).

Roles of the cytoplasmic tail and transmembrane domain of TMED7 in its intracellular localization

Next we wanted to address the link between TMED7's role in the intracellular trafficking of TLR4 and its signalling activity. First, we confirmed the intracellular localization of TMED7 shown by previous studies (*19, 24-26*) and determined whether the COP II sorting motif is required for this localization. THP-1 macrophages were transduced with the full length and truncated TMED7 constructs and the localization of these and the Golgi marker Giantin were visualized by immunofluorescent microscopy. As previously reported full length TMED7 is predominantly present in the Golgi as it co-localizes tightly with giantin (Fig. 7A). By contrast the Delta, CC, and GOLD truncations are not concentrated in the Golgi but are instead widely dispersed in the cytoplasm (Fig. 7B, C, and D). A similar pattern was observed in HEK293T cells transfected with C-terminally FLAG-tagged TMED7 or its truncated mutants (Fig. S7A). Further analysis in HEK293T cells using anti-protein disulphide isomerase (PDI), a marker for the ER, showed that while both CC and GOLD seem to overlap with PDI, Delta is distributed more diffusely and does not accumulate in the Golgi (Fig. S7B). Therefore it is evident that the cytosolic tail of TMED7 is essential for its correct localization within the Golgi as loss of the diphenylalanine motif causes the protein to be trapped in the endomembrane system.

TMED7 facilitates cell surface expression of TLR4

LPS stimulation of TLR4 can be initiated from either cell surface or in the Golgi following LPS internalization (*34, 35*). Therefore the cell surface expression level could determine the extent of LPS responsiveness observed above. N-glycosylation of TLR4 is important for cell surface expression and responsiveness to the ligand. Studies have shown that chaperone molecules are important for this process, as well as MD2, which is required for the glycosylation of TLR4 that enables the cell surface expression (*9, 12, 36*).

To assess the role of TMED7 in trafficking of TLR4 to the cell surface we used flow cytometry analysis performed on transfected HEK293T cells expressing FLAG-TLR4 and MD2, as well as on THP-1 macrophages expressing endogenous TLR4. Since the FLAG tag was located in the N-terminal of TLR4 ectodomain and the cells were not fixed nor permeabilized, only TLR4 molecules on the surface of HEK293T cells were observed in the assay. Viable cells

were gated based on forward and side scatter profile and this population was then analyzed for cells positive for Alexa Fluor 488 signal (TLR4) with the isotype control set as the signal threshold. Untransfected and unstained cells were included as negative controls to ensure that the signals were not due to non-specific antibody binding and auto-fluorescent cells, respectively. We used this method to measure the cell surface expression of TLR4 when the endogenous TMED7 level was knocked down with specific siRNA and when the protein was overexpressed. As shown in Fig. 8A, overexpression of transfected TMED7 leads to an increase in surface localized TLR4 receptors. By contrast knock-down of TMED7 in HEK293T cells led to a substantial reduction in the level of cell surface TLR4 based on percentage of transfected cells expressing cell surface TLR4 (Fig. 8B). These findings were validated by repeating the knock-down experiment in THP-1 macrophages. Knock-down of TMED7 caused a decrease in endogenous cell surface TLR4 and this was not due to decrease in gene expression of TLR4 (Fig. 8C and D).

Taken together these results indicate that TMED7 is involved in early stage trafficking of TLR4 leading to its transport to the cell surface and therefore positively regulates the signalling activity of the receptor.

DISCUSSION

In this paper we show that TLR4 is a cargo molecule for TMED7 a Golgi dynamics protein that facilitates the intracellular trafficking of the receptor prior to its transport to the cell surface. We present several lines of evidence that TMED7 is a type I membrane protein with a luminal N-terminal and a short cytoplasmic domain with characteristic di-phenylalanine COP II sorting motif (Fig. 1A and C). This topology for TMED7 (also called (g)p27 or p24γ3) is supported by historical studies, including N-terminal sequencing of native TMED7 isolated from Golgi membrane fractions of rat which reveals a cleaved signal peptide (*19*). Our conclusions are not, however, consistent with a recent study which reports that TMED7 is anchored in the membrane by the N-terminal helix and the GOLD domain is exposed to the cytoplasm (*32*). This conclusion was drawn from membrane fractionation assays by mutating each of the helical regions individually and protease protection assays although the experiment presented lacks a positive control to show that a bona fide ER lumen protein is protected from degradation under the conditions used. Doyle et al. also conclude that TMED7 interacts directly with the signalling

adaptor TRAM and a TMED7-TRAM splice hybrid (TRAM with GOLD domain (TAG)) (*37*), acting as negative regulator of the TLR4 signalling from the endosome. By contrast in this study we cannot detect a direct interaction between TMED7 and TRAM in unstimulated cells, a result that is consistent with the membrane topology and function we propose. In the case of TAG, a splicing product that includes the GOLD and coiled-coil domains of TMED7 joined to the TIR domain of TRAM, it may be that it is secreted and has a dominant negative effect by forming heterodimers with endogenous TMED7 in the ER lumen.

We have shown that the luminal coiled-coil and GOLD domains of TMED7 are sufficient to mediate binding of TLR4 and therefore it is likely the ectodomain of TLR4 that mediates binding. The GOLD domain alone does not form dimers and cannot bind to TLR4 suggesting that recognition requires homodimerization of TMED7 or heterodimerization with other TMED family members. It also establishes, as expected, that the domain predicted to form a α-helical coiled-coil mediates dimerization. The Delta and CC mutants which lack both the anterograde sorting signal for COP II also bind to TLR4 but do not accumulate in the Golgi. Thus it is likely that trafficking of TLR4 to the Golgi requires segregation into COP II coated vesicles by TMED homo-or hetero dimers and that association of TMED7 and TLR4 in a stable complex defines receptors that are transiting the early secretory pathway.

The presence of TRAM causes a substantial enhancement of TMED7 binding to TLR4. This could indicate that TRAM becomes pre-associated with TLR4 TIR domain during biosynthesis and this inhibits recognition of the COP II sorting motif and anterograde trafficking, leading to an accumulation of TMED7/TLR4 in the ER. In this regard previous studies show that TLR4 and TRAM co-localize in the Golgi and at the cell surface suggesting coordinated trafficking of the receptor and adaptor (*38*). TRAM is modified by the addition of the fatty acid myristate to an N-terminal glycine residue. The myristoyl group is added by the enzyme N-myristoyl transferase and the modified proteins are co-translationally inserted into the ER membrane (*39*). Thus another explanation for the observed accumulation of TMED7/TLR4 complexes might be that overexpression of TRAM sterically blocks the formation of the COP II coats required for anterograde transport, again causing the down regulation of ER to Golgi transport.

The expression of the Delta form of TMED7 enhances constitutive signalling to both IFNβ and NF-κB activation by about 20 fold suggesting that proper regulation of early stage

secretion is necessary to repress ligand-independent signalling that would produce potentially dangerous inflammatory responses. Lower levels of constitutive activation of about 2-5 fold are also observed when the wild type TMED7 and CC mutant are overexpressed, but not the GOLD domain alone. Constitutive activation of TLR4 can occur when the receptors accumulate in membranes to high concentrations. The TLR4 ectodomain acts as a constitutive suppressor of TLR4 activation and this repression can be relieved by exposure to ligand, overexpression, truncation or substitution with domains having a propensity for dimerization (*40*). In the case of CC the constitutive signal may originate from intracellular compartments as trafficking via the Golgi appears to be blocked, leading to accumulation of TLR4 intracellularly. On the other hand the activity caused by overexpressed full length TMED7 is probably the result of enhanced secretion of TLR4 to the cell surface (Fig. 8). Delta enhances signalling with and without the LPS which suggests that intracellular accumulation of TLR4 can drive an LPS-independent activation. Overall these results demonstrate a role for the di-phenylalanine COP II sorting motif in the cytosolic tail, and glutamic acid and glutamine residues in the transmembrane domain of TMED7 in TLR4 trafficking (*17, 19, 33*). These studies show that the interactions between these key residues not only affect the localization but also the rate of the anterograde trafficking of the TMED protein in a regulated manner (*33*).

It is interesting to note that while the overexpression of TMED7 affected both MyD88 and TRAM-dependent pathways, the knockdown only affected the MyD88-dependent pathway of TLR4 signalling. It is possible that this selectivity is caused by the fact that these two pathways are initiated from two distinct locations—the cell surface and early endosomes (*2, 5*). Kagan et al. proposed the sequential initiation of MyD88-dependent pathway on the cell surface followed by endocytosis and initiation of TRAM-dependent pathway in the early endosomes. The model put forward by Husebye et al. showed that there are two distinct TLR4 populations on the cell surface and in the endocytic recycling compartment (ERC) of human monocytes that can respond to *E. coli* infection independently of each other. From these conclusions, we can postulate that whilst initiation of MyD88-dependent pathway upon TLR4 stimulation relies on the transport of the receptor to the cell surface, the activation of TRAM-dependent pathway relies on both the endocytosis of activated receptor and the trafficking of naive TLR4 in the ERC to the ligand-containing phagosome which is Rab11a-dependent. Therefore, the main role of TMED7 is to traffick TLR4 to the cell surface and not to the other intracellular compartments

such as the ERC. This explains why TMED7 depletion only affects the MyD88-dependent pathway from the cell surface.

Little is known about the molecular mechanisms by which TMED proteins associate with their cargoes in the ER. However the available evidence suggests that secretion is coupled to the addition of N-linked glycans in the ER. For example a systematic mutagenesis of potential N-glycosylation sites in TLR2 showed that all four are modified and contribute to efficient secretion, although a conserved site at the C-terminus is of particular importance (*41*). In the case of TLR4 there are nine N-glycans and two of these, N526 and N575, are essential for secretion with other sites having a more partial effect on cell surface expression (*12*). Thus an attractive hypothesis is that TMED7, acting as a quality control step, assembles with TLR4 by recognising the nascent glycosylated receptor in the ER lumen and marking the receptor as cargo for anterograde transport in COP II vesicles to ERGIC and Golgi compartments.

Another aspect of interest is the release mechanism of TLR4 from TMED7 in the Golgi. Recently Rab10 was identified to promote TLR4 trafficking to the cell surface from the Golgi (*15*). It is therefore possible that TMED7 and Rab10 work together in the process of TLR4 transport to the cell surface. However, the precise molecular events that lead to this have not been elucidated yet. The acidic pH of the compartment in the late secretory pathway could lead to the dissociation between TMED and its cargo protein (*42*), a similar general mechanism also operates to cause release of LDL from its receptor after internalization into acidic endosomes (*43*). A more tightly regulated switch could be implemented such as that used by TMED2 in the resensitization of protease-activated receptor (PAR) 2 on the cell surface from the Golgi (*44*). In the resting state, TMED2 associates with its PAR2 cargo in the Golgi. Upon stimulation of PAR2 on the cell surface, the receptors are endocytosed and the cell surface has to be replenished with new populations of the receptor. This event is mediated by the activation of a small GTP-binding protein ADP-ribosylation factor (ARF) 1 that leads to the dissociation of PAR2 from TMED2. This could explain the decrease in the amount of TMED7 associated with the TLR4 upon LPS stimulation in HEK293T cells (Fig. 2C). Perhaps a similar mechanism is employed in this particular system to resensitize the TLR4 receptors.

In future studies we aim to explore the nature of the interactions between TMED dimers and TLR ectodomain glycans at a molecular level and test the hypothesis that disassembly of

TLR4 in the Golgi is mediated by the transition to low pH and Golgi specific modification of the glycans.

MATERIALS AND METHODS

Constructs, and antibodies

Human TLR4 and human CD14 in pcDNA3, human MD2 in pEFIRES, and p125 -luc were generously provided by Dr Clare Bryant, University of Cambridge, UK. p125-luc contains the promoter region of IFN-β followed by firefly luciferase as described previously (*45*). phRG-TK and pNF-κB-luc were purchased from Promega and Clontech respectively. TRAM with C-terminal FLAG and His tags (TRAM-FLAG) in pEF-BOS, TLR4 with N-terminal FLAG tag (FLAG-TLR4) were gifts from Dr Ashley Mansell, MIMR, Australia. TMED7-GFP in EX-V1709-M03 (OmicsLink) was a gift from Prof. Luke O'Neill, Trinity College Dublin, Ireland. pHR: TLR4Cit and pHR: TLR3Cit with C-terminal mCitirine tag were gifts from Dr Brett Verstak.

Primary antibodies used in this study were anti-HA produced in rabbit and in chicken (abcam, ab9110 and ab9111 respectively), anti-FLAG produced in mouse (Sigma, F3165), IgG1 isotype control from murine myeloma (Sigma, M5284), anti-giantin produced in rabbit (abcam, ab24586), anti-PDI antibody [RL77]-ER marker produced in mouse (abcam, ab5484), anti-human CD284 (TLR4) PE (eBioscience, 12-9917), and mouse IgG2a K isotype control PE (eBioscience, 12-4724) . Secondary antibodies used in this study were anti-rabbit IgG (whole molecule)-peroxidase produced in goat (Sigma, A0545), anti-mouse IgG (whole molecule)-peroxidase produced in goat (Sigma, A4416), Mouse TrueBlot ULTRA: anti-mouse Ig HRP (eBioscience, 18-8817) for Western blotting. For immunofluorescence, Alexa Fluor 633 goat anti-chicken IgG (H+L) (Molecular Probes, A21103), and Alexa Fluor 405 goat anti-rabbit IgG (H+L) (Molecular Probes, A31556), and Alexa Fluor 488 goat anti-mouse IgG (H+L) (Molecular Probes, A11001).

Cloning and mutagenesis

Mammalian expression vectors of human TMED7 and its truncated mutants were constructed using TMED7-GFP in EX-V1709-M03 as the template using Gateway cloning technology (Invitrogen). Standard PCR reactions were performed using Vent polymerase (NEB). The constructs created were called TMED7 (full length, 1-224), CC (1-187), and GOLD (1-144). attB1 and attB2 sites were incorporated into the forward and reverse primers respectively, flanking the gene, for cloning into the pDONR221 entry vector by Gateway BP reaction using BP clonase enzyme. One forward primer contained an attB1 site followed by the native signal peptide of TMED7 in 5′-3′ direction. Three reverse primers, for each of the three constructs, consisted of an attB2 site, stop codon, FLAG or HA tag, and followed by TMED7 gene specific sequence in 5′-3′ direction. Gateway LR reaction was then performed using LR clonase enzyme to insert the gene into a Gateway pcDNA-DEST47 destination vector ready for expression in mammalian cells.

Another mutant of TMED7, Delta (1-210, lacking the cytoplasmic tail) with C-terminal HA, was created by Quikchange mutagenesis using PfuTurbo (Stratagene). Primer pairs for mutagenesis were designed to skip the cytoplasmic tail to be deleted, using TMED7-HA previously made as a template in the PCR reaction. See Supplementary Materials for primer sequences (Tables S1 and 2).

For lentivirus production, genes of interest were cloned into pHR vector. Briefly, PCR reactions were carried out to amplify the genes of interest and to incorporate a BamH1 and a Not1 restriction sites at the 5′ and 3′ ends of the gene respectively. Both the PCR products and pHR:TLR4Cit were treated with BamH1 and Not1 restriction enzymes (NEB, R3136 and R3189) according to the manufacturer's protocol and purified. Ligation reactions were carried out using T4 DNA Ligase (NEB, M202). See Supplementary Materials for protocol for lentivirus production.

Cell culture and DNA transfection

HEK293 and HEK293T cells were grown in Dulbecco's Modified Eagle's Medium (DMEM) (Sigma, D5546). The media was supplemented with 2 mM L-glutamine, 100 units/ml penicillin, 100 µg/ml streptomycin, and 10% (v/v) heat-inactivated foetal calf serum (FCS) at 37°C, 5% CO_2. jetPEI transfection reagent (Polyplus transfection) was used for DNA plasmid transfection according to the manufacturer's protocol. A total of 100 ng of DNA plasmid was transfected per

well in a 96-well plate. For cells grown on a 6-well plate, a total of 3 μg of DNA plasmid were transfected per well. For detailed accounts of the amount of DNA transfected for different assays, see Tables S3-5. Cells were analyzed 24-48 hours post-transfection.

THP-1 monocyte was from Dr Clare Bryant. The cells were maintained in suspension in RPMI-1640 with L-glutamine and sodium bicarbonate (Sigma, R8758), supplemented with 10% FCS, 100 units/ml penicillin, 100 μg/ml streptomycin, 25 mM HEPES, and 20 μM β-mercaptoethanol. Prior to siRNA transfection, THP-1 monocytes had to be differentiated into THP-1 macrophages. For differentiation, cells were treated with 100 ng/ml phorbol myristate acetate (PMA) (Sigma, P8139) in complete RPMI for two days prior to subsequent analysis.

siRNA transfection, RNA extraction, and qPCR

siRNA duplexes targeting TMED7 were purchased from Invitrogen (Stealth siRNA HSS121495, or siRNA95 for short) and from Sigma (siRNA2 and 3). siRNA2 and 3 duplexes were designed in our lab using siRNA target finder tool from Ambion. Generated sequences were subsequently ranked using parameters described in (*46*) and only two sequences with the highest scores were selected, see Table S6 for sequences of the siRNA duplexes. siRNA transfection into HEK293/ 293T cells was performed using jetPRIME transfection reagent (Polyplus transfection) per well and incubated for three days prior to consequent DNA transfection or data collection. siRNA transfection into THP-1 macrophages was performed using INTERFERin (Polyplus transfection) two days after PMA treatment, and cells were incubated for three more days prior to subsequent analyses by ELISA or flow cytometry.

Total RNA from cells were purified using RNeasy Plus kit and QiaShredder (QIAgen). First strand cDNA was synthesized from the total RNA using SuperScript II reverse transcriptase (Invitrogen) with random hexamer (Promega, C1181) as described in the protocol from Untegasser lab (http://www.untergasser.de/lab/protocols/cdna_synthesis_superscript_ii_v1 _0.htm).

The cDNA served as template for real time quantitative PCR (qPCR) analysis to determine the level of gene knockdown using Platinum SYBR Green qPCR SuperMix (Invitrogen, 11733038). Relative gene level of TMED7 was determined and normalized against internal control of GAPDH (for HEK293T) or β-Actin (for THP-1 macrophages) to determine the relative gene knockdown using Livak method of $2^{(-\Delta\Delta Ct)}$. The gene-specific primers for

TMED7, TRAM, TLR4, β-Actin, and GAPDH were designed to span the exon-exon junction to eliminate amplification of genomic DNA (Table S7).

Luciferase reporter assay

The protocol was adapted from a previously described method (*47*). Briefly, HEK293 cells were transfected with appropriate expression vectors using jetPEI transfection reagent. Reporter genes used were p125-luc and pNF-κB-luc. For knockdown experiment, siRNA was transfected three days prior to DNA transfection as described above. 48 hours after the DNA transfection, cells were stimulated with LPS from *E. coli* O127:B8 (Sigma Aldrich, L3129), Poly I:C HMW (Inivogen, tlrl-pic), or flagellin from *S. typhimurium* (Invivogen, tlrl-stfla) diluted in serum-free DMEM for 6 hours. The cells were washed in PBS and then lysed using passive lysis buffer (Promega) diluted in PBS. Firefly and *Renilla* luciferase activities were quantified individually using luciferin and coelenterazine reagents respectively using LUMIstar Omega luminometer (BMG Labtech).

Enzyme-linked immunosorbent assay

Three days post siRNA transfection into THP-1 macrophages, the cells were stimulated with LPS diluted in serum-free RPMI-1640 for 24 hours at concentrations indicated in the figures. The amount of human IL-6, TNFα, and RANTES cytokines produced upon LPS stimulation was measured in the culture supernatant following the protocol from R&D systems ELISA kit.

Co-immunoprecipitation and Western blot analysis

48-72 hours following transfection or transduction, cells were lysed in cold lysis buffer (50 mM Tris-HCl, pH 7.6, 150 mM NaCl, 1 mM EDTA, 2 mM $MgCl_2$, 2 mM $CaCl_2$) containing 1% Triton X-100, 0.5% n-Octylglucoside, and supplemented with 1 mM PMSF and 1x protease inhibitor cocktail set V (Calbiochem, 535141). Soluble extract of cell lysate was collected by centrifugation at 15000 g for 10 min. FLAG-tagged recombinant proteins in the rest of the supernatant were immunoprecipitated by incubation with anti-FLAG M2 magnetic beads (Sigma, M8823, using DynaMag-2 magnet (Invitrogen) to separate beads from wash buffer. Total protein and co-immunoprecipitated samples were analyzed by Western blot using antibodies as indicated in figures.

Enzymatic deglycosylation

Protein was harvested from HEK293T cells in lysis buffer as described above, but with 1% NP-40 detergent only. TMED7-HA from cell lysate was treated with 1000 U PNGaseF (NEB) following the manufacturer's protocol, or just the buffers for negative control for overnight at 37°C. SDS loading buffer with reducing agent was added to the beads and boiled at 100°C for 10 min. Samples were analyzed by Western blot.

Confocal microscopy

Cells were seeded on coverslips on a 6-well plate. Two-three days after transfection or transduction, the media was aspirated off from the wells, and cells on the coverslips were washed once in cold phosphate buffer saline (PBS). The cells were then fixed using 4% paraformaldehyde in PBS and permeabilized with 0.2% Triton x-100 in PBS at room temperature. Cells were washed twice between steps in cold PBS. For immunohistostaining, cells were blocked in blocking buffer (5% BSA in PBS with 0.1% Tween-20 (PBST)) for 30 min at room temperature. Cells were stained in a cocktail of primary antibodies against HA produced in chicken and Giantin produced in rabbit (all diluted 1:200 in blocking buffer) for overnight in fridge. Cells were then washed three times in PBST before incubated in a cocktail of Alexa Fluor-conjugated secondary antibodies against chicken (AF633), and rabbit (AF405) (all diluted 1:200 in blocking buffer) for 1 hour at room temperature. Coverslips were then inversely mounted onto glass SuperFrost Plus 76x26mm glass slides (VWR International) containing two drops of Vectashield hardset mounting medium (Vectorlabs). Leica SP5 Upright (Laser wavelengths used: 405 nm, 514 nm, and 633 nm) was used to visualize the cells. Leica LAS AF software was used to obtain the fluorescent micrographs.

Flow cytometry

Two days after transfection, HEK293T cells were detached from the bottom of the wells with accutase (PAA) and washed once in PBS and blocked in blocking buffer (5% BSA in PBS) for 30 min at room temperature. Cells were stained with 10 µg/ml anti-FLAG antibody or mouse IgG1 isotype control in blocking buffer for O/N in fridge, washed and then incubated with

secondary antibody conjugated to Alexa Fluor 488 for 1 hour at room temperature in dark. Cells were washed and analyzed on BD Accuri C6 flow cytometer.

Three days after siRNA transfection, THP-1 macrophages were detached from the bottom of the wells with cold 10 mM EDTA in PBS and were washed once in 0.5% BSA in PBS and blocked in blocking buffer for 30 min at room temperature. Cells were stained in anti-CD284 (TLR4) PE (2 µg/ test) or mouse IgG2a K isotype control PE (0.5 µg/ test) in blocking buffer for O/N in the fridge. Cells were washed twice and analyzed on BD Accuri C6 flow cytometer.

Statistical analysis

All graphs were generated using Prism5 (GraphPad) and the statistical analyses were performed using unpaired, two-tailed t test with Welch's correction to obtain the p-values where appropriate.

REFERENCES AND NOTES

1. C. E. Bryant, D. R. Spring, M. Gangloff, N. J. Gay, The molecular basis of the host response to lipopolysaccharide. *Nat. Rev. Microbiol.* **8**, 8 (2010).
2. J. C. Kagan, T. Su, T. Horng, A. Chow, S. Akira, R. Medzhitov, TRAM couples endocytosis of Toll-like receptor 4 to the induction of interferon-beta. *Nat. Immunol.* **9**, 361 (2008).
3. J. C. Kagan, R. Medzhitov, Phosphoinositide-mediated adaptor recruitment controls Toll-like receptor signaling. *Cell* **125**, 943 (2006).
4. I. Zanoni, R. Ostuni, L. R. Marek, S. Barresi, R. Barbalat, G. M. Barton, F. Granucci, J. C. Kagan, CD14 controls the LPS-induced endocytosis of Toll-like receptor 4. *Cell* **147**, 868 (2011).
5. H. Husebye, M. H. Aune, J. Stenvik, E. Samstad, F. Skjeldal, O. Halaas, N. J. Nilsen, H. Stenmark, E. Latz, E. Lien, T. E. Mollnes, O. Bakke, T. Espevik, The Rab11a GTPase controls Toll-like receptor 4-induced activation of interferon regulatory factor-3 on phagosomes. *Immunity* **33**, 583 (2010).
6. H. Husebye, O. Halaas, H. Stenmark, G. Tunheim, O. Sandanger, B. Bogen, A. Brech, E. Latz, T. Espevik, Endocytic pathways regulate Toll-like receptor 4 signaling and link innate and adaptive immunity. *EMBO J.* **25**, 683 (2006).
7. L. A. O'Neill, A. G. Bowie, The family of five: TIR-domain-containing adaptors in Toll-like receptor signalling. *Nat. Rev. Immunol.* **7**, 353 (2007).
8. K. Takahashi, T. Shibata, S. Akashi-Takamura, T. Kiyokawa, Y. Wakabayashi, N. Tanimura, T. Kobayashi, F. Matsumoto, R. Fukui, T. Kouro, Y. Nagai, K. Takatsu, S. Saitoh, K. Miyake, A protein associated with Toll-like receptor (TLR) 4 (PRAT4A) is required for TLR-dependent immune responses. *J. Exp. Med.* **204**, 2963 (2007).
9. Y. Wakabayashi, M. Kobayashi, S. Akashi-Takamura, N. Tanimura, K. Konno, K. Takahashi, T. Ishii, T. Mizutani, H. Iba, T. Kouro, S. Takaki, K. Takatsu, Y. Oda, Y.

Ishihama, S. Saitoh, K. Miyake, A protein associated with toll-like receptor 4 (PRAT4A) regulates cell surface expression of TLR4. *J. Immunol.* **177**, 1772 (2006).
10. F. Randow, B. Seed, Endoplasmic reticulum chaperone gp96 is required for innate immunity but not cell viability. *Nat. Cell. Biol.* **3**, 891 (2001).
11. Y. Nagai, S. Akashi, M. Nagafuku, M. Ogata, Y. Iwakura, S. Akira, T. Kitamura, A. Kosugi, M. Kimoto, K. Miyake, Essential role of MD-2 in LPS responsiveness and TLR4 distribution. *Nat. Immunol.* **3**, 667 (2002).
12. J. da Silva Correia, R. J. Ulevitch, MD-2 and TLR4 N-linked glycosylations are important for a functional lipopolysaccharide receptor. *J. Biol. Chem.* **277**, 1845 (2002).
13. T. Ohnishi, M. Muroi, K. Tanamoto, MD-2 is necessary for the toll-like receptor 4 protein to undergo glycosylation essential for its translocation to the cell surface. *Clin. Diagn. Lab. Immunol.* **10**, 405 (2003).
14. T. L. Gioannini, A. Teghanemt, D. S. Zhang, N. P. Coussens, W. Dockstader, S. Ramaswamy, J. P. Weiss, Isolation of an endotoxin-MD-2 complex that produces Toll-like receptor 4-dependent cell activation at picomolar concentrations. *Proc. Natl. Acad. Sci. U S A* **101**, 4186 (2004).
15. D. Wang, J. Lou, C. Ouyang, W. Chen, Y. Liu, X. Liu, X. Cao, J. Wang, L. Lu, Ras-related protein Rab10 facilitates TLR4 signaling by promoting replenishment of TLR4 onto the plasma membrane. *Proc. Natl. Acad. Sci. U S A* **107**, 13806 (2010).
16. F. Brandizzi, C. Barlowe, Organization of the ER-Golgi interface for membrane traffic control. *Nature Rev. Mol. Cell Biol.* **14**, 382 (2013).
17. K. Fiedler, M. Veit, M. A. Stamnes, J. E. Rothman, Bimodal interaction of coatomer with the p24 family of putative cargo receptors. *Science* **273**, 1396 (1996).
18. F. Kappeler, D. R. Klopfenstein, M. Foguet, J. P. Paccaud, H. P. Hauri, The recycling of ERGIC-53 in the early secretory pathway. ERGIC-53 carries a cytosolic endoplasmic reticulum-exit determinant interacting with COPII. *J. Biol. Chem.* **272**, 31801 (1997).
19. M. Dominguez, K. Dejgaard, J. Fullekrug, S. Dahan, A. Fazel, J. P. Paccaud, D. Y. Thomas, J. J. M. Bergeron, T. Nilsson, gp25L/emp24/p24 protein family members of the cis-Golgi network bind both COP I and II coatomer. *J. Cell Biol.* **140**, 751 (1998).
20. J. Dancourt, C. Barlowe, Protein Sorting Receptors in the Early Secretory Pathway. *Annu. Rev. Biochem.* **79**, 777 (2010).
21. J. R. Strating, N. H. van Bakel, J. A. Leunissen, G. J. Martens, A comprehensive overview of the vertebrate p24 family: identification of a novel tissue-specifically expressed member. *Mol. Biol. Evol.* **26**, 1707 (2009).
22. J. R. Strating, G. J. Martens, The p24 family and selective transport processes at the ER-Golgi interface. *Biol. Cell.* **101**, 495 (2009).
23. K. Sohn, L. Orci, M. Ravazzola, M. Amherdt, M. Bremser, F. Lottspeich, K. Fiedler, J. B. Helms, F. T. Wieland, A major transmembrane protein of Golgi-derived COPI-coated vesicles involved in coatomer binding. *J. Cell. Biol.* **135**, 1239 (1996).
24. J. Fullekrug, T. Suganuma, B. L. Tang, W. J. Hong, B. Storrie, T. Nilsson, Localization and recycling of gp27 (hp24 gamma(3)): Complex formation with other p24 family members. *Mol. Biol. Cell* **10**, 1939 (1999).
25. G. Emery, M. Rojo, J. Gruenberg, Coupled transport of p24 family members. *J. Cell Sci.* **113**, 2507 (2000).
26. N. Jenne, K. Frey, B. Brugger, F. T. Wieland, Oligomeric state and stoichiometry of p24 proteins in the early secretory pathway. *J. Biol. Chem.* **277**, 46504 (2002).

27. M. A. Stamnes, M. W. Craighead, M. H. Hoe, N. Lampen, S. Geromanos, P. Tempst, J. E. Rothman, An integral membrane component of coatomer-coated transport vesicles defines a family of proteins involved in budding. *Proc. Natl. Acad. Sci. U S A* **92**, 8011 (1995).
28. M. Marzioch, D. C. Henthorn, J. M. Herrmann, R. Wilson, D. Y. Thomas, J. J. Bergeron, R. C. Solari, A. Rowley, Erp1p and Erp2p, partners for Emp24p and Erv25p in a yeast p24 complex. *Mol. Biol. Cell* **10**, 1923 (1999).
29. W. J. Belden, C. Barlowe, Deletion of yeast p24 genes activates the unfolded protein response. *Mol. Biol. Cell* **12**, 957 (2001).
30. A. Denzel, F. Otto, A. Girod, R. Pepperkok, R. Watson, I. Rosewell, J. J. M. Bergeron, R. C. E. Solari, M. J. Owen, The p24 family member p23 is required for early embryonic development. *Curr. Biol.* **10**, 55 (2000).
31. L. A. Jerome-Majewska, T. Achkar, L. Luo, F. Lupu, E. Lacy, The trafficking protein Tmed2/p24beta(1) is required for morphogenesis of the mouse embryo and placenta. *Dev. Biol.* **341**, 154 (2010).
32. S. L. Doyle, H. Husebye, D. J. Connolly, T. Espevik, L. A. J. O'Neill, A. F. McGettrick, The GOLD domain-containing protein TMED7 inhibits TLR4 signalling from the endosome upon LPS stimulation. *Nat. Commun.* **3**, 707 (2012).
33. K. Fiedler, J. E. Rothman, Sorting determinants in the transmembrane domain of p24 proteins. *J. Biol. Chem.* **272**, 24739 (1997).
34. M. W. Hornef, B. H. Normark, A. Vandewalle, S. Normark, Intracellular recognition of lipopolysaccharide by toll-like receptor 4 in intestinal epithelial cells. *J. Exp. Med.* **198**, 1225 (2003).
35. E. Latz, A. Visintin, E. Lien, K. A. Fitzgerald, B. G. Monks, E. A. Kurt-Jones, D. T. Golenbock, T. Espevik, Lipopolysaccharide rapidly traffics to and from the Golgi apparatus with the toll-like receptor 4-MD-2-CD14 complex in a process that is distinct from the initiation of signal transduction. *J. Biol. Chem.* **277**, 47834-47843 (2002).
36. F. Rocuts, Y. Ma, X. Zhang, W. Gao, Y. Yue, T. Vartanian, H. Wang, Carbon monoxide suppresses membrane expression of TLR4 via myeloid differentiation factor-2 in betaTC3 cells. *J. Immunol.* **185**, 2134-2139 (2010).
37. E. M. Palsson-McDermott, S. L. Doyle, A. F. McGettrick, M. Hardy, H. Husebye, K. Banahan, M. Gong, D. Golenbock, T. Espevik, L. A. O'Neill, TAG, a splice variant of the adaptor TRAM, negatively regulates the adaptor MyD88-independent TLR4 pathway. *Nat. Immunol.* **10**, 579-586 (2009).
38. D. C. Rowe, A. F. McGettrick, E. Latz, B. G. Monks, N. J. Gay, M. Yamamoto, S. Akira, A. O'Neill L, K. A. Fitzgerald, D. T. Golenbock, The myristoylation of TRIF-related adaptor molecule is essential for Toll-like receptor 4 signal transduction. *Proc. Natl. Acad. Sci. U S A* **103**, 6299-6304 (2006).
39. D. R. Johnson, R. S. Bhatnagar, L. J. Knoll, J. I. Gordon, Genetic and biochemical studies of protein N-myristoylation. *Annu. Rev. Biochem.* **63**, 869 (1994).
40. G. Panter, R. Jerala, The ectodomain of the Toll-like receptor 4 prevents constitutive receptor activation. *J. Biol. Chem.* **286**, 23334 (2011).
41. A. N. Weber, M. A. Morse, N. J. Gay, Four N-linked glycosylation sites in human toll like receptor 2 cooperate to direct efficient biosynthesis and secretion. *J. Biol. Chem.* **279**, 34589-34594 (2004).

42. M. Fujita, R. Watanabe, N. Jaensch, M. Romanova-Michaelides, T. Satoh, M. Kato, H. Riezman, Y. Yamaguchi, Y. Maeda, T. Kinoshita, Sorting of GPI-anchored proteins into ER exit sites by p24 proteins is dependent on remodeled GPI. *J. Cell Biol.* **194**, 61 (2011).
43. G. Rudenko, L. Henry, K. Henderson, K. Ichtchenko, M. S. Brown, J. L. Goldstein, J. Deisenhofer, Structure of the LDL receptor extracellular domain at endosomal pH. *Science* **298**, 2353-2358 (2002).
44. W. Luo, Y. Wang, G. Reiser, p24A, a type I transmembrane protein, controls ARF1-dependent resensitization of protease-activated receptor-2 by influence on receptor trafficking. *J. Biol. Chem.* **282**, 30246 (2007).
45. M. Yoneyama, W. Suhara, Y. Fukuhara, M. Sato, K. Ozato, T. Fujita, Autocrine amplification of type I interferon gene expression mediated by interferon stimulated gene factor 3 (ISGF3). *J. Biochem.* **120**, 160 (1996).
46. A. Reynolds, D. Leake, Q. Boese, S. Scaringe, W. S. Marshall, A. Khvorova, Rational siRNA design for RNA interference. *Nat. Biotechnol.* **22**, 326 (2004).
47. C. Walsh, M. Gangloff, T. Monie, T. Smyth, B. Wei, T. J. McKinley, D. Maskell, N. Gay, C. Bryant, Elucidation of the MD-2/TLR4 interface required for signaling by lipid IVa. *J. Immunol.* **181**, 1245 (2008).
48. M. Lewis, C. J. Arnot, H. Beeston, A. McCoy, A. E. Ashcroft, N. J. Gay, M. Gangloff, Cytokine Spatzle binds to the Drosophila immunoreceptor Toll with a neurotrophin-like specificity and couples receptor activation. *Proc. Natl. Acad. Sci. U S A* **110**, 20461 (2013).
49. A. N. Weber, M. Gangloff, M. C. Moncrieffe, Y. Hyvert, J. L. Imler, N. J. Gay, Role of the Spatzle Pro-domain in the generation of an active toll receptor ligand. *J. Biol. Chem.* **282**, 13522 (2007).
50. G. Emery, J. Gruenberg, M. Rojo, The p24 family of transmembrane proteins at the interface between endoplasmic reticulum and Golgi apparatus. *Protoplasma* **207**, 24 (1999).

Figures and Tables

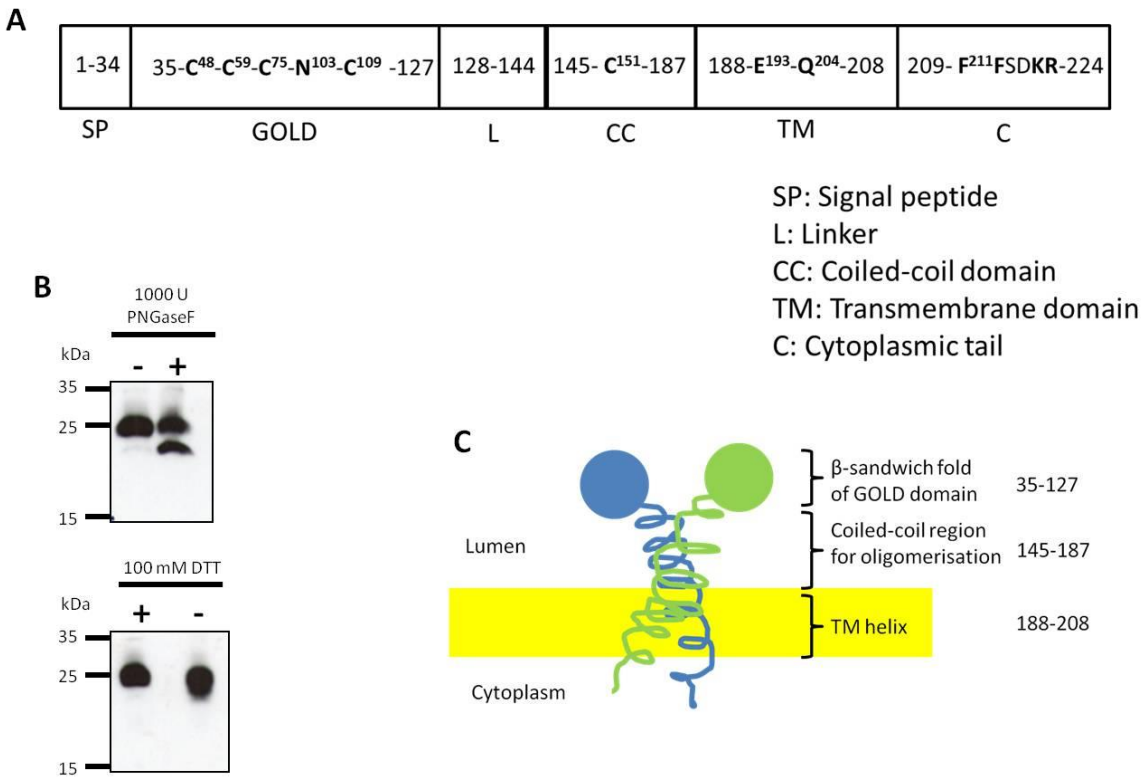

Figure 1. Characterization of TMED7 protein organization. (**A**) Summary of domain arrangement of TMED7, based on various prediction tools and previous studies (*19*, *24*, *44*, *50*) with their residue position numbers indicated in the domain boxes. Cysteine 48 and 109 are absolutely conserved in all members of the p24 family across all species studied whereas the other cysteine residues are highly conserved (*22*). Asparagine 103 is predicted to be a site of N-glycosylation. Glutamate 193 and glutamine 204 are sorting signals within the transmembrane domain that modulate the vesicular trafficking activity of TMED7 (*33*). Di-phenylalanine residues in the cytoplasmic tail is a motif involved in COP II binding (*19*). (**B**) TMED7-HA was transiently transfected in HEK293T cells. The whole cell lysate was collected and was analyzed for TMED7 glycosylation state by PNGaseF treatment, and for the presence of any disulfide bridges by treatment with reducing agent DTT. Western blot was performed using anti-HA antibody. Data is representative of N=2. (**C**) Cartoon representation of domain organization and topology of TMED7 with its N-terminal GOLD domain located within the lumen.

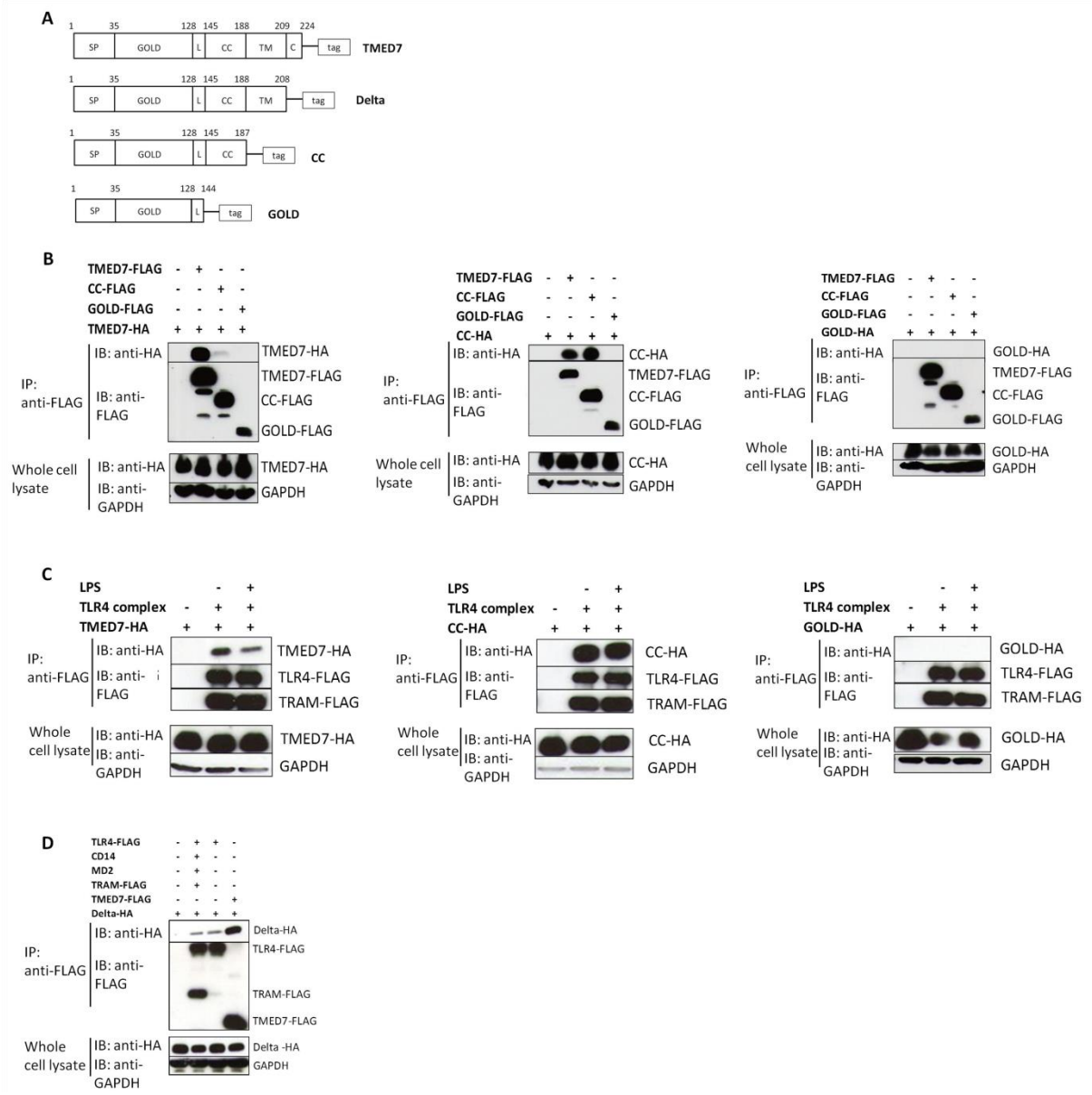

Figure 2. Oligomerization of TMED7 is crucial for interaction with TLR4. (**A**) Constructs of full length TMED7 and its truncated mutants (Delta, CC, and GOLD) with C-terminal tag used in this study. SP: signal peptide; GOLD: Golgi dynamics domain; L: linker; CC: coiled-coil domain; TM: transmembrane domain; C: cytoplasmic tail. (**B**) TMED7 and its truncated mutants were tested for oligomerization in co-immunoprecipitation (co-IP) assay. HEK293T cells were transiently transfected with plasmids as indicated in the panel and the whole cell lysate was incubated with anti-FLAG M2 magnetic beads to immunoprecipitate FLAG-tagged recombinant proteins, and anti-HA antibody was used to detect the interacting HA-tagged protein. Anti-FLAG antibody was used to detect the presence of the immunoprecipitated bait, and GAPDH was detected as a loading control. (**C**) TMED7 and its truncated mutants were tested for interaction with TLR4 receptor complex (FLAG-TLR4, MD2, CD14, and TRAM-FLAG) with 100 ng/ml LPS stimulation for 30 min. (**D**) TMED7 lacking cytoplasmic tail (Delta) is still capable of forming an oligomer with full length TMED7 and interacting with TLR4. Data are representative of N=3.

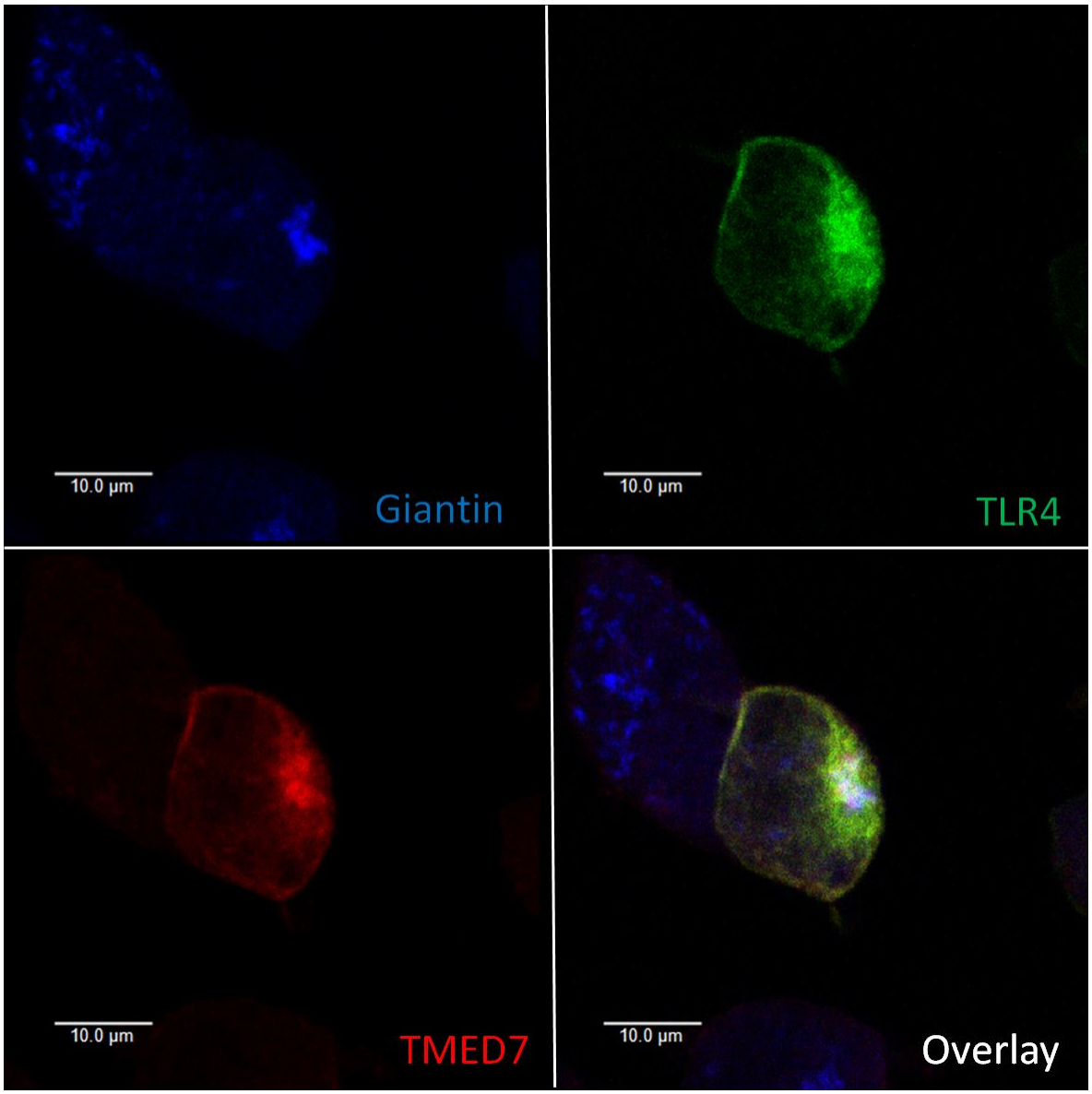

Figure 3. TLR4 and TMED7 co-localization in HEK293T cells without LPS stimulation. Cells were transiently transfected with TMED7-HA, TLR4-Citrine, MD2, CD14, and TRAM. 48 hours post-transfection cells were permeabilized and TMED7-HA was labelled with AlexaFluor633 (red), and Giantin was detected with AlexaFluor405 (blue). Data is representative of two independent experiments where around 20 cells from each experiment were observed to have similar pattern.

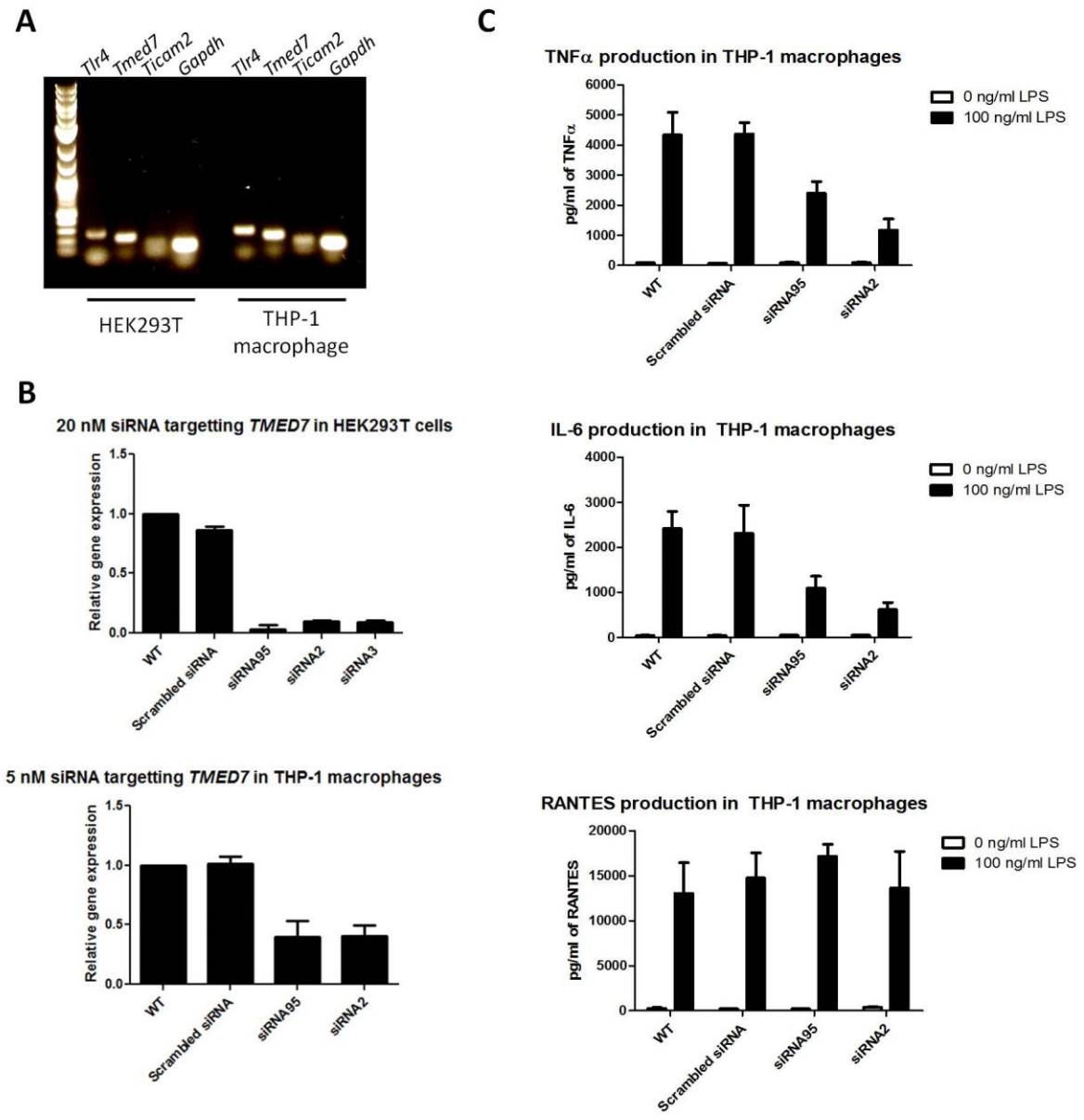

Figure 4. TMED7 knockdown in THP-1 macrophages reduced expression of IL-6 and TNFα cytokines upon LPS stimulation. (A) Determination of endogenous gene expression of TMED7 in HEK293T and THP-1 macrophages by RT-PCR. Total RNA was purified and the cDNA was synthesized by reverse transcription. The cDNA was used as template for PCR analysis using gene specific primers. (**B**) Efficiency of various siRNA duplexes targeting TMED7 in HEK293T (top) and THP-1 macrophages (bottom) were measured by qPCR 3 days post siRNA transfection. TMED7 gene expression level is normalised against GAPDH or β-Actin and shown as relative expression to wild type (WT). (**C**) Cytokine measurement by ELISA of TNFα (top), IL-6 (middle) and RANTES (bottom) produced by THP-1 macrophages. Upon differentiation to THP-1 macrophages, cells were transfected with various siRNA duplexes and incubated for three days. Cells were then stimulated with 100 ng/ml LPS for 24 hours prior to cytokine measurement by ELISA. Data are from one representative experiment of N=3, error bars represent standard deviation.

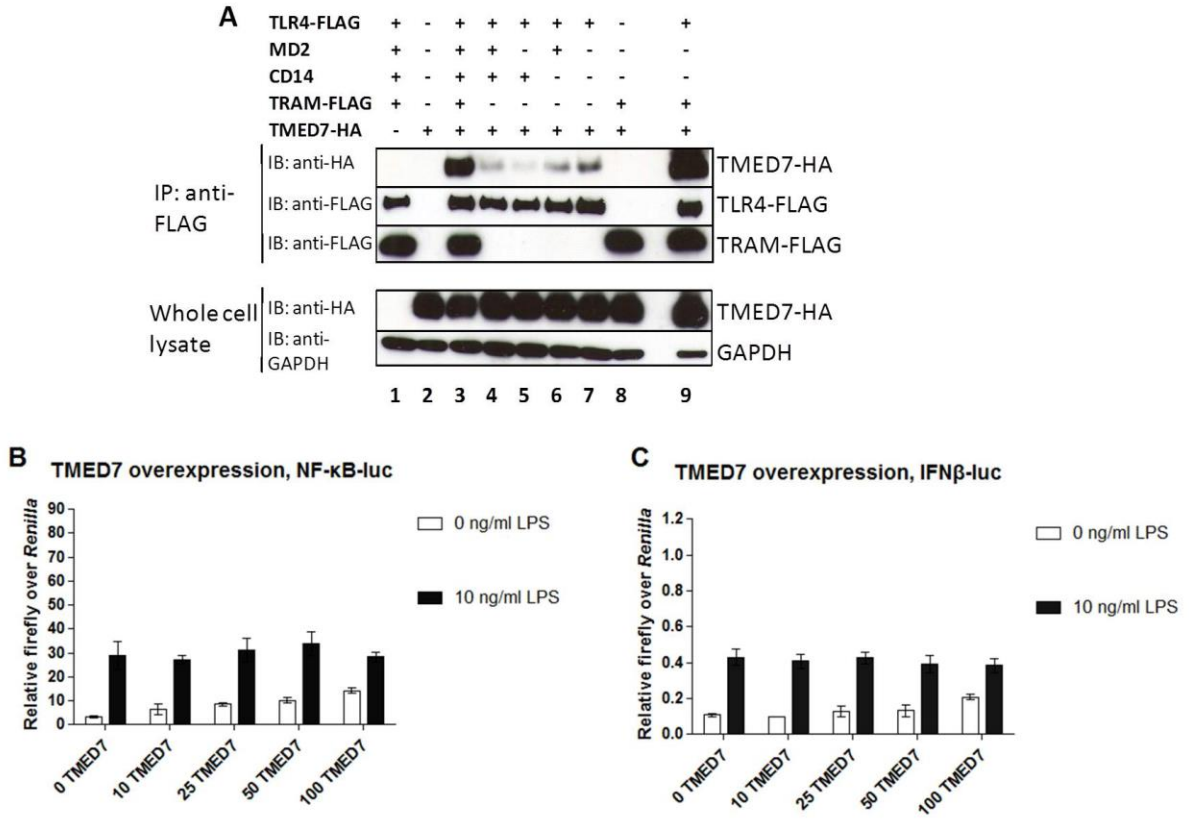

Figure 5. Figure 4. TMED7 regulates TLR4 signalling pre-LPS stimulation. (**A**) TLR4 on its own is sufficient to interact with TMED7. HEK293T cells were transiently transfected with plasmids as indicated in the panel. Without LPS stimulation, the whole cell lysate was incubated with anti-FLAG M2 magnetic beads to immunoprecipitate FLAG-tagged recombinant proteins, and anti-HA antibody was used to detect the interacting HA-tagged protein. Anti-FLAG antibody was used to detect the presence of the immunoprecipitated bait, and GAPDH was detected as a loading control. Figure is representative of N=3. (**B** and **C**) TMED7's role on TLR4 signalling was investigated using reporter luciferase assay in constituted HEK293 cells. TMED7-HA overexpression increased the basal level of TLR4 activations of (**B**) NF-κB and (**C**) IFN-β in the absence of LPS, but LPS-stimulated activation of TLR4 remained unaffected. Data is presented as firefly luciferase activity normalized against *Renilla* luciferase activity on Y-axis, and the amount of TMED7 in ng transfected per 10 wells of 96-well plate on X-axis. Data is from a representative experiment of N=5. Error bars represent standard deviation.

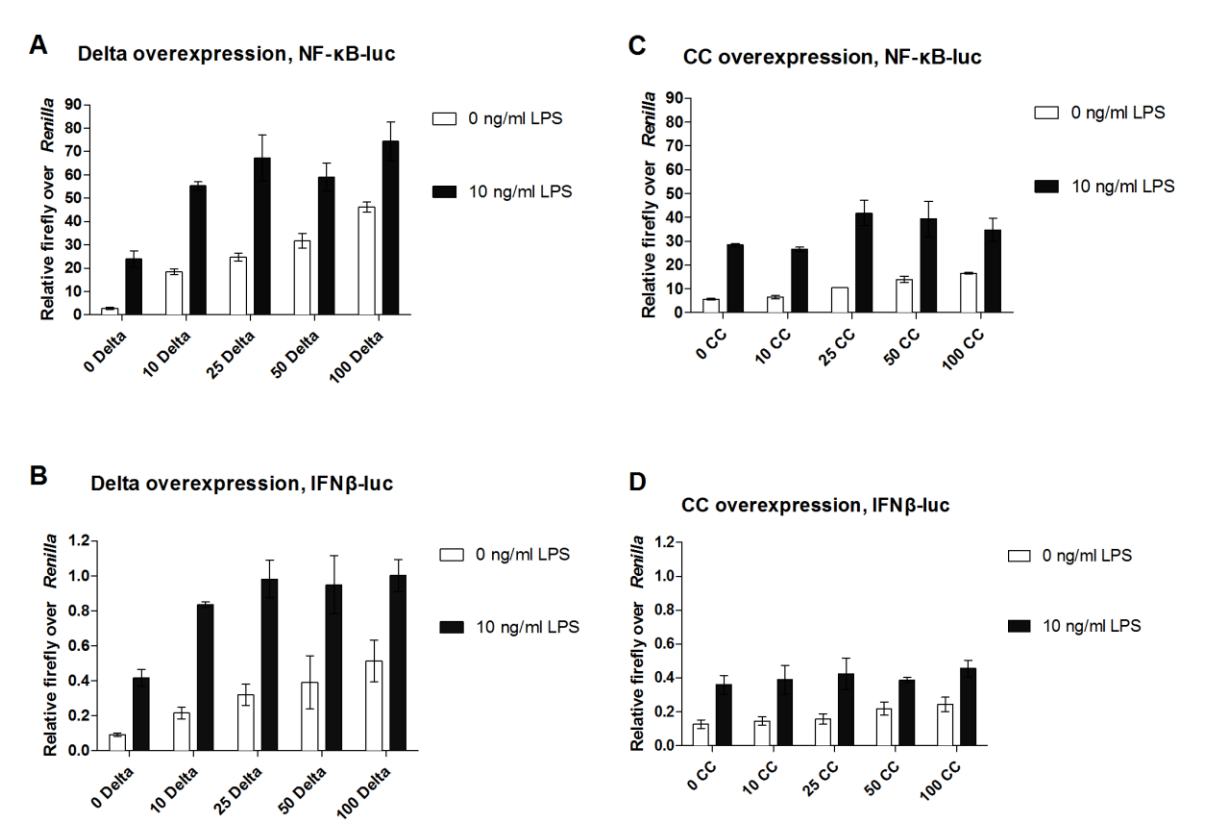

Figure 6. Roles of the transmembrane and cytosolic tail of TMED7 in TLR4 signalling. Loss of the cytoplasmic tail of TMED7 (Delta) caused a drastic increase in both NF-κB, and IFNβ activations even at LPS-stimulated state (**A** and **B**), whereas CC behaved similarly to full length TMED7 (**C** and **D**). Data is presented as firefly luciferase activity normalized against *Renilla* luciferase activity on Y-axis, and the amount of Delta-HA or CC-HA plasmid in ng transfected per 10 wells of 96-well plate on X-axis. Data is from a representative experiment of N=5. Error bars represent standard deviation.

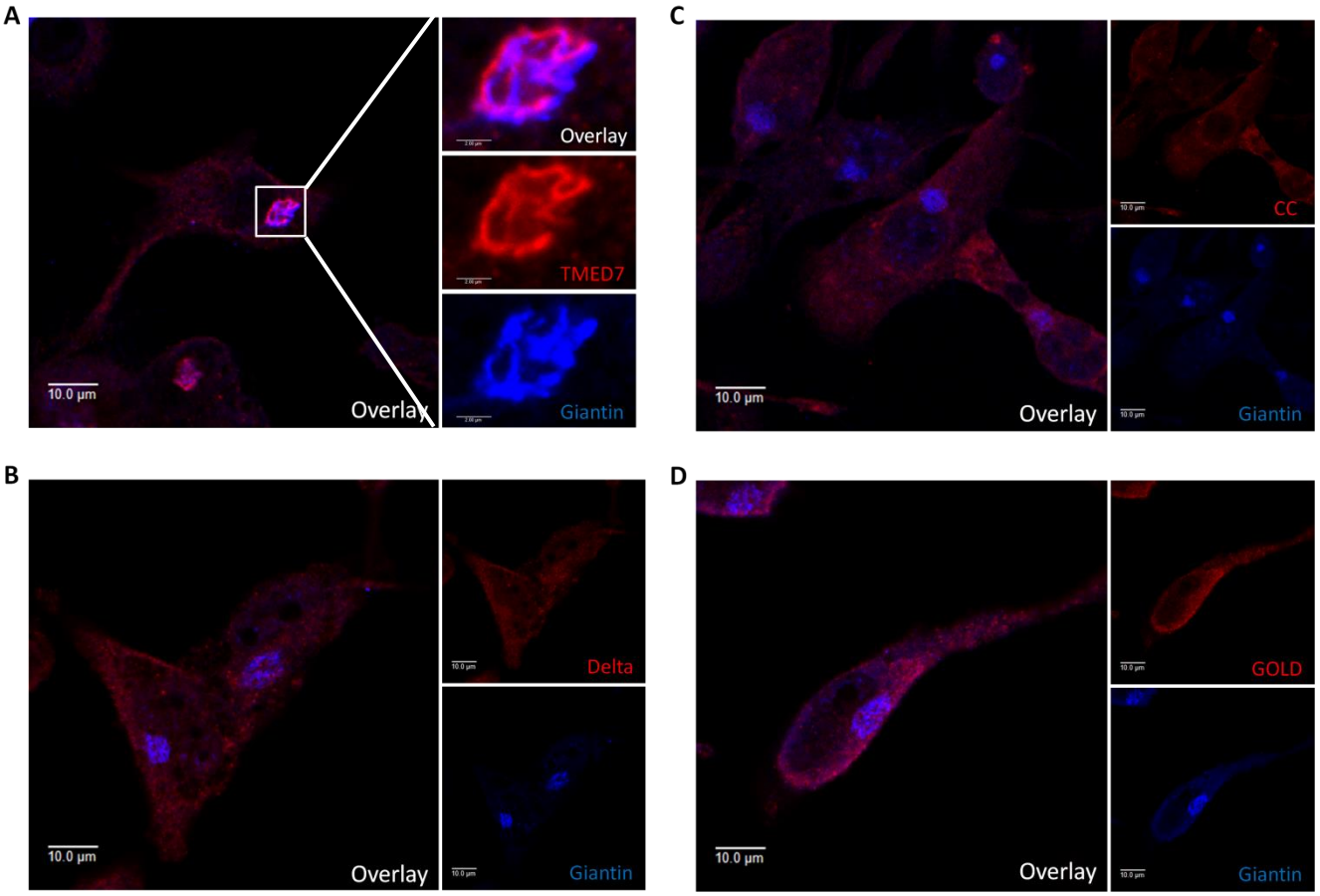

Figure 7. Localization of TMED7 in the Golgi in THP-1 macrophages is due to the COP II-binding motif. THP-1 macrophages were transduced with lentivirus and incubated for three days. The cells were permeabilized and HA-tagged TMED7, Delta, CC and GOLD were labelled with AlexaFluor633 (red) whereas endogenous Giantin was labelled with AlexaFluor404 (blue). The presence of the di-phenylalanine residues in the cytosolic tail of TMED7 determine its localization in the Golgi together with Giantin (**A**). Loss of the motif leads to loss of distinct localization of TMED7 in the Golgi (**B**, **C**, and **D**). Data is representative of two independent experiments where around 20 cells from each experiment were observed to have similar pattern.

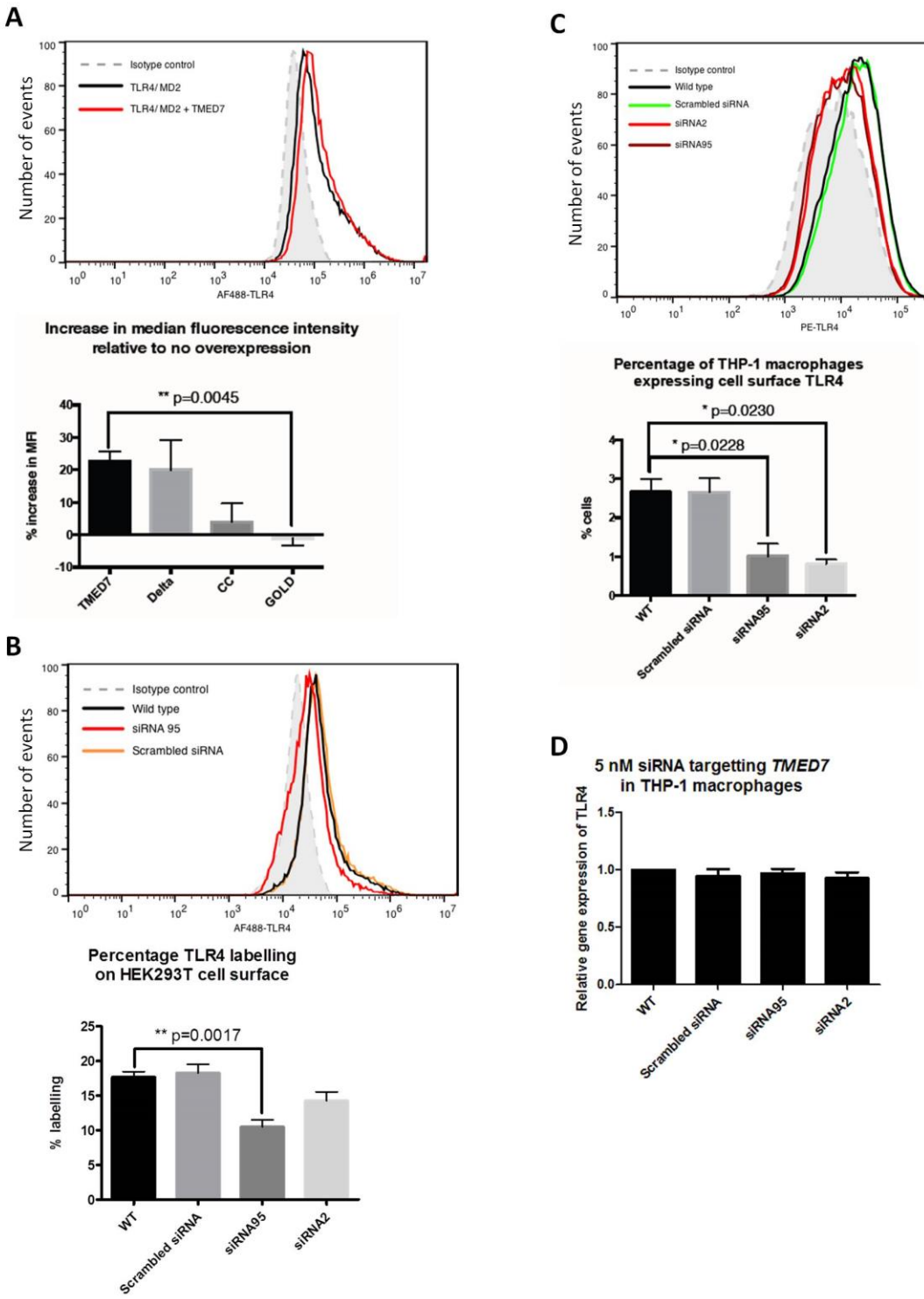

Figure 8. TMED7 enhances cell surface expression of TLR4. Flow cytometric analysis cell surface expression of transfected TLR4 in HEK293T cell and endogenous TLR4 in THP-1 macrophages. (**A**) TMED7 overexpression increases FLAG-TLR4 expression on HEK293T cell surface. Histogram shows the shift upon TMED7-HA overexpression (compare red and black lines), bottom panel represents the increase in median fluorescence intensity (MFI) of cell surface TLR4 staining relative to no overexpression. (**B**) TMED7 knock-down in HEK293T cells decreases cell surface expression of transfected FLAG-TLR4 (compare red and black lines). Bottom panel shows

percentage of TLR4 labelling after the siRNA treatment, cell population stained by isotype control antibody was set as the basal level in the quadrant gating. (**C** and **D**) TMED7 knock-down in THP-1 macrophages decreases cell surface endogenous TLR4 but not the total amount of TLR4. (**D**) Relative gene expression of TLR4 after 3-day siRNA treatment determined by qPCR. Histogram data are representative N=3. MFI, %labelling, and relative gene expression data are averaged results from three independent experiments error bars represent standard error of mean, p-values were calculated using unpaired, two-tailed t test with Welch's correction.